

ARTICLE

DOI: 10.1038/s41467-017-00192-5

OPEN

Zhamanshin astrobleme provides evidence for carbonaceous chondrite and post-impact exchange between ejecta and Earth's atmosphere

Tomáš Magna¹, Karel Žák², Andreas Pack³, Frédéric Moynier^{4,5}, Bérengère Mougel⁴, Stefan Peters³, Roman Skála², Šárka Jonášová², Jiří Mizera⁶ & Zdeněk Řanda⁶

Chemical fingerprints of impacts are usually compromised by extreme conditions in the impact plume, and the contribution of projectile matter to impactites does not often exceed a fraction of per cent. Here we use chromium and oxygen isotopes to identify the impactor and impact-plume processes for Zhamanshin astrobleme, Kazakhstan. $\epsilon^{54}\text{Cr}$ values up to 1.54 in irghizites, part of the fallback ejecta, represent the ^{54}Cr -rich extremity of the Solar System range and suggest a CI-like chondrite impactor. $\Delta^{17}\text{O}$ values as low as -0.22‰ in irghizites, however, are incompatible with a CI-like impactor. We suggest that the observed ^{17}O depletion in irghizites relative to the terrestrial range is caused by partial isotope exchange with atmospheric oxygen ($\Delta^{17}\text{O} = -0.47\text{‰}$) following material ejection. In contrast, combined $\Delta^{17}\text{O}$ - $\epsilon^{54}\text{Cr}$ data for central European tektites (distal ejecta) fall into the terrestrial range and neither impactor fingerprint nor oxygen isotope exchange with the atmosphere are indicated.

¹Czech Geological Survey, Klárov 3, Prague 1 CZ-118 21, Czech Republic. ²Institute of Geology of the Czech Academy of Sciences, v.v.i., Rozvojová 269, Prague 6 CZ-165 00, Czech Republic. ³Geowissenschaftliches Zentrum, Abteilung Isotopengeologie, Universität Göttingen, Goldschmidtstraße 1, Göttingen D-37077, Germany. ⁴Institut de Physique du Globe de Paris, Université Paris Diderot, 1 rue Jussieu, Paris F-75005, France. ⁵Institut Universitaire de France, Paris F-75005, France. ⁶Nuclear Physics Institute of the Czech Academy of Sciences, v.v.i., Husinec-Řež CZ-250 68, Czech Republic. Correspondence and requests for materials should be addressed to T.M. (email: tomas.magna@geology.cz)

Large-scale planetary collisions and smaller impacts are important processes that may add to the chemical makeup of the bodies in the Solar System and shape the planetary surfaces by forming variably sized craters, layers of impact ejecta, and shock deformation features. Some meteorites, in particular carbonaceous chondrites, contain high concentrations of organic matter and volatiles like water, and are considered to potentially bear on the emergence of oceans and life¹. The identification of projectile types for impacts is thus central for tracing the origin and aftermath of collisions. In general, chondrites are regarded as the most frequent projectiles in larger impacts² (see also ref. ³ for the recent summary of meteorite types and individual numbers of specimens). High thermal energy that is released in impacts leads to almost complete melting and/or evaporation of the impactor as well as large amount of the target rocks, and may also change the behavior of the elements and their chemical compounds⁴, making the identification of the projectile difficult.

Tektites (distal ejecta) and other impact-related glasses (part of proximal and fallback ejecta) are natural glassy materials which are genetically related to hypervelocity impacts of large extra-terrestrial bodies on the Earth's surface. They are produced by intense melting and partial evaporation of the target materials during the impact event, and may bear traces of the impactor^{5,6}. Tektites are found as variably shaped and sized objects; typically, they are of splash-form shapes with a size of few centimetres. They usually are interpreted as being formed from the uppermost layers of the target lithologies, i.e., unconsolidated sediments and soils, partly vaporized and partly melted and ejected with a high velocity from the boundary zone between the impactor and the Earth's surface by jetting⁷. They are mostly silica-rich and with extremely low contents of volatile components (H₂O, C, S, halogens, etc.). In fact, tektites belong to the most volatile-depleted natural materials on Earth, often with <100 p.p.m. H₂O^{8–10} and low contents of other volatiles (<30–40 p.p.m. C)¹¹. There is not an agreement on the exact formation mechanisms of tektites and several concepts have been published^{4, 12–14}. A general model of tektite formation and volatile loss^{12, 14, 15} developed the original ideas¹⁶ considering possible mechanisms of fragmentation of the overheated tektite melt by separating vapor phase^{17, 18}. These ideas were further developed for tektites of the Central European tektite field (moldavites)⁴. This latter conceptual model of formation of tektites considers two main pathways of the behavior of the ejected supercritical fluid during adiabatic decompression: (i) the supercritical matter approaches the sub-critical vapor/melt boundary from the vapor phase stability field and most matter is vaporized, or (ii) the less energetic part of the ejected matter reaches the vapor/melt boundary from the melt stability field and a directly formed overheated melt is fragmented due to separation of the vapor phase (cf. Fig. 1 in refs ^{17, 18}). The melt fragmentation can strongly be amplified by the escape of water-, carbonate- and/or organic matter-based volatiles derived from the target, which were effectively lost from the tektite melts^{9, 11}. Immediate coalescence (accretion) of small melt droplets into larger tektite bodies, probably underscored by formation of late condensation spherules, appears to be the most viable process which may explain the general chemical homogeneity of tektites, in parallel to their large micro-scale chemical heterogeneity, and the general absence of condensation and/or inner diffusion profiles in tektite bodies⁴.

Oxygen isotope (¹⁶O, ¹⁷O, ¹⁸O) ratios have been used to classify asteroidal and planetary materials in the Solar System¹⁹ and O isotopes could thus be used to help identify the impactor. Large mass-independent fractionation (MIF) of oxygen isotopes has been recognized for different Solar System bodies most likely inherited from MIF processes during early Solar System formation, whereas common terrestrial and other planetary materials

(e.g., Mars, Moon, Vesta) have ¹⁸O/¹⁶O and ¹⁷O/¹⁶O ratios which are solely fractionated by mass-dependent processes^{20, 21}. The only isotopically anomalous components of Earth are found in the atmosphere. Molecular oxygen has a distinctly negative $\Delta^{17}\text{O}$ anomaly²² (see Methods for definition of $\Delta^{17}\text{O}$) that is mainly caused by biological processes (i.e., photosynthesis, respiration), and by minor effects of photochemical reactions in the upper atmosphere²³. Due to high temperatures of impact ejecta at the time of formation and during atmospheric re-entry, O isotope anomalies in tektites and related glasses could also be caused by partial post-impact exchange with the Earth's atmosphere²⁴ although this process has not yet been reported for truly terrestrial samples. In fact, small negative $\Delta^{17}\text{O}$ offsets (as low as -0.18‰) were reported for some tektites²⁰ but it remains unclear whether these low values could provide evidence for such a process or, alternatively, for the presence of impactor material with low $\Delta^{17}\text{O}$ values.

The utility of chromium isotope (⁵⁰Cr, ⁵²Cr, ⁵³Cr, ⁵⁴Cr) systematics to characterize the impactor type was proven in several cases, including the Chicxulub impact at the Cretaceous–Paleogene boundary². Distinct planetary bodies and meteorite groups show resolved differences in the ⁵³Cr/⁵²Cr and ⁵⁴Cr/⁵²Cr ratios^{25, 26}, underscored by particularly high Cr abundance in chondrites, compared to the terrestrial continental crust. Because individual chondrite groups have distinctive ¹⁷O–⁵⁴Cr isotope fingerprints³, combined O–Cr isotope measurements may allow identification of impactor material and distinction between impactor- or atmospheric exchange-related variations in $\Delta^{17}\text{O}$.

To test the viability of O–Cr isotopes to constrain the impactor type for tektites and impact-related glasses, we measured triple-oxygen isotope compositions for a set of 14 impact-related tektite-like glasses from the Zhamanshin astrobleme (basic splash forms, and acid splash forms—irghizites, two chemically disparate groups of impact-related glasses), and 14 Central European tektites (moldavites), related to the Ries impact event in Germany. Chromium isotope compositions were obtained for two

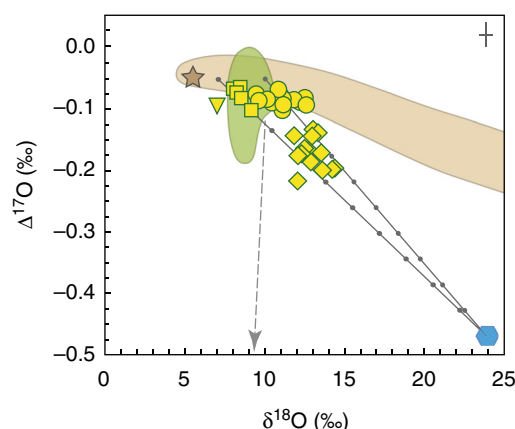


Fig. 1 Oxygen isotope systematics in tektites and impact glasses from this study. Mixing lines between siliciclastic and mafic materials ($\delta^{18}\text{O} = 10.0\text{‰}$ and 7.0‰ , respectively) and air O₂ are indicated, *bullets* represent 10‰ increments. *Circles*—moldavites; *diamonds*—irghizites; *squares*—basic splash forms; *reversed triangle*—composite splash-form; *brown field*—the range of common crustal rocks⁵⁴ with revised data for San Carlos olivine⁷⁶; *green field*—the recalculated oxygen isotope compositions of other tektites²⁰ (Australasian tektites, North American tektites). The oxygen isotope compositions of the Earth's mantle (star)⁷⁶ and air (hexagon)²² are plotted. Carbonaceous chondrite groups other than CI have more negative $\Delta^{17}\text{O}$ values (*dashed arrow*). The maximum 2 s.d. error bars for $\delta^{18}\text{O}$ and $\Delta^{17}\text{O}$ are plotted

impact-related glasses from Zhamanshin, one moldavite, and terrestrial BHVO-2 reference basalt. The detailed analytical procedures for O and Cr isotope measurements and notations for O and Cr isotope compositions are detailed in the Methods section. All samples were previously characterized for major and trace element systematics^{4, 27, 28}.

Zhamanshin and Ries differ in the size of impactor (estimated diameter of ~0.6 km vs. ~1.2–1.5 km)^{27, 29}, paleogeography (dry vs. wet area) and indications of the presence vs. absence of extraterrestrial addition in some types of impactites. The Zhamanshin impactor is interpreted to have been about one order of magnitude lower in mass than that of the Ries impact event and it probably was below the size limit necessary for production of distal ejecta, i.e., true tektites. In addition, taking into account the distribution of proximal ejecta, trajectories of both projectiles differed; in case of Zhamanshin the impact must have been much steeper²⁷ than in case of a relatively shallow trajectory of the Ries projectile^{12, 30}. The target surface conditions of Zhamanshin and Ries were also different. While the target of the Ries impact event in the Miocene was a wet area near the limit of the Miocene Upper Freshwater Molasse ('Obere Süßwassermolasse'—OSM) sedimentary basin³¹, probably densely overgrown by forests, dry and possibly cold desert conditions are to be expected during the Quaternary in central Asia²⁷. Therefore, the quantity of volatiles (derived from H₂O, organic carbon, etc.) produced during the Zhamanshin impact can be estimated to be more than one order of magnitude lower than in the case of Ries. The compressed and ejected material of shallow layers of Zhamanshin target thus did not travel to a great distance. Instead, the glass droplets which formed from disintegrated near-surface melts were falling back through the explosion plume and collected small particles both of the mechanically disintegrated impactor matter and condensed particles from the portion of the matter which was evaporated. These glass droplets then coalesced together to form irghizites^{27, 28}. In a number of cases, the surface layers of primary droplets within irghizites are strongly enriched in Fe, Mg, Cr, Co, Ni and P^{28, 32}.

We explore several types of glasses from the Zhamanshin impact structure (48°24'N/60°58'E), all belonging to the fallback and proximal ejecta. The major focus of the study is on tektite-like splash-form glassy objects sized usually up to several centimetres. Three major chemical types are distinguished: (i) SiO₂-rich (usually 69–76 wt.% SiO₂) irghizites^{33, 34} which have commonly been formed by coalescence of < 1 mm glass droplets and have elevated concentrations of Ni, Co and Cr^{27, 28}, (ii) morphologically rather uniform drops and their fragments composed of more basic glass, termed 'basic splash forms' (53–56 wt.% SiO₂)^{27, 28, 32, 35–38}, and (iii) composite splash forms, defined as inhomogeneous acidic splash forms with abundant mineral inclusions²⁸. Impact glasses occurring in larger irregularly shaped fragments and large blocks called 'zhamanshinites'³³ were not the subject of this study because earlier studies excluded any presence of the impactor matter in these objects²⁸. We refer to the Supplementary Note 1 for further details.

Tektites of the Central European strewn field (moldavites) are genetically related to the Ries Impact Structure, Germany (48° 53'N/10°33'E), a complex type astrobleme with a diameter of ~26 km³⁹. Unconsolidated sandy, silty and clayey sediments of the OSM, probably covering most of the target area at the time of the impact, are generally considered to be the dominant source material of moldavites^{4, 13, 29, 30, 39–46}. The origin of moldavites in relation to the Ries Impact Structure has also been confirmed by generally consistent ages of moldavites and impact-related glasses from the Ries Impact Structure itself at 14.75 ± 0.20 Ma^{31, 47}. The nature of the impactor remains elusive^{48, 49} due to difficulties in finding unequivocal extraterrestrial chemical signatures both in moldavites and impact-related glasses⁵⁰.

Table 1 Oxygen isotope composition of impact-related materials from this study

	$\delta^{18}\text{O}$ (‰) ^a	$\delta^{17}\text{O}$ (‰)	$\Delta^{17}\text{O}$ (‰) ^a	n
<i>Tektites</i>				
SBM-11	11.18	5.83	−0.088	1
SBM-11 replicate ^b	9.62	5.02	−0.090	1
SBM-23	10.98	5.72	−0.080	1
SBM-35	12.46	6.50	−0.084	2
SBM-44	10.95	5.71	−0.086	2
SBM-88	12.57	6.55	−0.096	3
SBM-192	11.79	6.15	−0.085	1
MM-60	10.85	5.65	−0.092	2
MM-67	10.84	5.66	−0.070	1
CHBM-5	11.81	6.15	−0.086	2
CHBM-6	9.44	4.92	−0.078	1
CHBM-7 ^b	10.13	5.30	−0.086	2
MCB-2	12.14	6.33	−0.091	2
LM-1	11.10	5.79	−0.085	2
MOLD-SB ^b	11.08	5.30	−0.105	1
MOLD-SB replicate ^b	10.45	5.79	−0.092	1
MOLD-SB replicate ^b	11.12	5.47	−0.095	1
<i>Irghizites</i>				
IRG-IZ1	12.76	6.58	−0.170	2
IRG-IZ3	11.85	6.12	−0.145	2
IRG-IZ3 replicate	13.36	6.92	−0.141	1
IRG-IZ3 replicate	13.05	6.76	−0.135	1
IRG-IZ3 replicate ^b	12.98	6.76	−0.147	1
IRG-IZ9	14.42	7.42	−0.198	2
IRG-IZ9 replicate ^b	13.59	7.03	−0.201	1
IRG-IZ9 replicate ^b	13.49	7.01	−0.173	1
IR-2	14.24	7.33	−0.200	1
IR-4	12.30	6.33	−0.175	1
IR-8	12.49	6.44	−0.166	1
IR-9	12.09	6.18	−0.219	1
IR-11	12.90	6.63	−0.188	1
IR-12	12.10	6.22	−0.178	1
<i>Basic splash forms</i>				
IRG-M4	8.01	4.17	−0.068	2
IRG-M4 replicate	9.18	4.76	−0.104	1
IR-10	8.47	4.42	−0.066	1
IR-13	8.26	4.30	−0.075	1
IR-14	8.56	4.45	−0.084	1
<i>Composite splash forms</i>				
IR-7	7.03	3.63	−0.094	1

^aEstimated measurement uncertainties are <0.3‰ and <0.008‰ for $\delta^{18}\text{O}$ and $\Delta^{17}\text{O}$, respectively, based on the typical reproducibility (1 s.d.) of results for the standard reference material NBS 28 throughout the analytical sessions, except for samples denoted with superscript 'b'

^bSamples analyzed with an improved extraction line (see text for details). Estimated measurement uncertainties are <0.15‰ and <0.007‰ for $\delta^{18}\text{O}$ and $\Delta^{17}\text{O}$, respectively, based on the typical reproducibility (1 s.d.) of measurement results for San Carlos olivine

Results

Oxygen isotopes. The $\Delta^{17}\text{O}$ values of moldavites (from −0.11 to −0.07‰; Table 1) overlap with crustal rocks (Fig. 1) and the range of $\delta^{18}\text{O}$ values from 9.4 to 12.6‰ exceeds that reported previously (from 10.7 to 11.9‰)^{41, 51–53}. The larger variability in $\delta^{18}\text{O}$ likely is a consequence of analyzing a chemically more variable suite of moldavites^{4, 29}. The new data set confirms the ~3–5‰ offset in $\delta^{18}\text{O}$ between moldavites and unconsolidated OSM quartz-rich sands (Fig. 2), where the likely major moldavite source material analogs such as bulk Miocene sediments from southern surroundings of the Ries Impact Structure showed distinctly higher and more variable $\delta^{18}\text{O}_{\text{SMOW}}$ values from 14.1 to 23.3‰ (ref. 41). The OSM sands, which are assumed to be the dominant source for moldavites^{4, 41}, showed $\delta^{18}\text{O}$ values from 14.1 to 16.5‰ with an average of 15.3‰ (ref. 41) and the predominance of sands in moldavites is also reflected in low MgO and CaO contents and moderate $\delta^{18}\text{O}$ (Fig. 3), excluding large

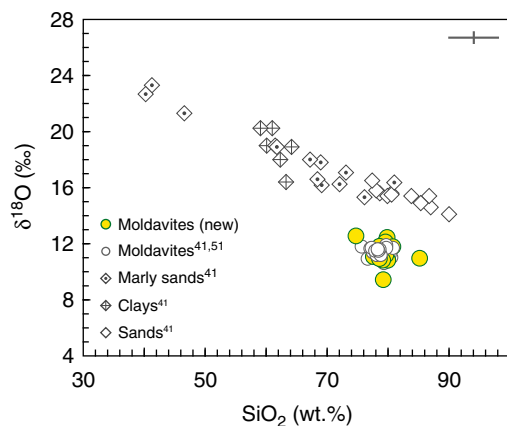


Fig. 2 New and published $\delta^{18}\text{O}$ values vs. SiO_2 contents in moldavites and sediments from the Ries area. The wider range in $\delta^{18}\text{O}$ values of moldavites from this study is due to analyzing chemically more variable specimens²⁹ compared to those analyzed earlier^{41, 51}. Silica contents in some earlier analyzed moldavites⁵¹ were reported elsewhere⁸³. Available combined SiO_2 - $\delta^{18}\text{O}$ data for chemically diverse Ries area sediments⁴¹ are plotted. Clays and marly sands can represent only a small proportion of parental material to moldavites while SiO_2 -rich sands dominate the budget^{4, 13, 41}. The consistent $\delta^{18}\text{O}$ offset of ~ 3 – 5% between moldavites and possible parental sediments from Ries area appears to be a combination of several aspects, explored in detail in the main text. The maximum 2 s.d. error bars for $\delta^{18}\text{O}$ ($\pm 0.4\%$) and SiO_2 ($\pm 2\%$) are plotted

volumes of carbonates in moldavite melts. The basic splash forms from Zhamanshin show $\Delta^{17}\text{O}$ values (-0.10 to -0.07%) that also overlap with crustal rocks. The $\Delta^{17}\text{O}$ values measured for irghizites ($-0.22 \leq \Delta^{17}\text{O} \leq -0.14\%$) are significantly lower than those measured for basic splash forms, for the moldavites, and also those reported for common crustal rocks (ref. ⁵⁴ and discussion therein; Fig. 1). This difference is underscored by distinct $\delta^{18}\text{O}$ values for basic splash forms and irghizites (8.0 – 9.2% vs. 11.9 – 14.4%). The $\Delta^{17}\text{O} = -0.09\%$ for composite splash-form IR-7 is at the low end of values for a given $\delta^{18}\text{O} = 7.0\%$ (Fig. 1).

Chromium isotopes. Irghizite IR-8 and composite splash-form IR-7 display a significant positive anomaly in ^{54}Cr ($\epsilon^{54}\text{Cr}$ up to 1.54) which is clearly outside the terrestrial range (Fig. 4) and indicates extraterrestrial origin of a large part of Cr^{27, 28} in IR-8 and IR-7. This is different from the results for moldavite SBM-88 and basalt BHVO-2 (Table 2), which are indistinguishable from typical terrestrial values^{26, 55, 56}.

Discussion

Moldavites have uniform terrestrial $\Delta^{17}\text{O}$ values (mean $\Delta^{17}\text{O} = -0.09 \pm 0.02\%$, 2 s.d.) that are consistent with common sedimentary precursors and weathered residues^{4, 41} (Fig. 1). This indicates insignificant contamination by isotopically anomalous extraterrestrial matter. Neither is any exchange with air O_2 obvious. The absence of any apparent evidence for impactor material is underscored by Cr isotope data for the slightly Cr-enriched⁵⁷ moldavite SBM-88 with $\epsilon^{54}\text{Cr} = 0.09 \pm 0.07$ (2 s.e.), which is identical to the values reported for a range of pristine terrestrial materials⁵⁶ (Table 2). Because Cr is a sensitive tracer of chondritic contamination in impact-related materials^{2, 58}, the new coupled ^{17}O - ^{54}Cr isotope data support the lack of extraterrestrial addition for moldavites outside the currently achievable analytical precision for these elements.

The consistent negative $\delta^{18}\text{O}$ offset of ~ 3 – 5% found for moldavites relative to the Ries area target rocks is extended for a

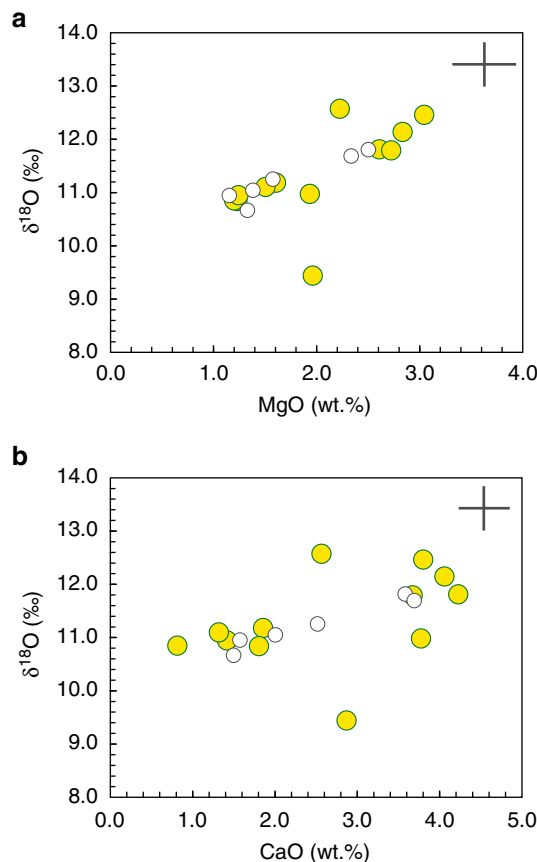


Fig. 3 New and published $\delta^{18}\text{O}$ values vs. MgO **a** and CaO **b** in moldavites. The wider range in $\delta^{18}\text{O}$ values from this study (yellow circles) is not reflected in distinctive major element compositions⁴, compared with other published data^{51, 83}. The 2 s.d. error bars are plotted

larger chemical range of moldavites, analyzed in this study (Fig. 2; this study and refs. ^{41, 51}), and requires mass-dependent ^{18}O depletion (Fig. 1). This offset can generally be interpreted by either addition of a low- $\delta^{18}\text{O}$ component, or additional mass-dependent O isotope fractionation during tektite formation^{41, 59}. To explain this several per mil offset, incorporation and isotope homogenization of ~ 22 vol.% of a low- $\delta^{18}\text{O}$ water (-10%) partly filling ~ 40 – 45 vol.% of pore spaces of the OSM sands, followed by conversion of the matter to plasma and its condensation back to a silicate glass was advocated^{13, 41}. However, to shift the $\delta^{18}\text{O}_{\text{SMOW}}$ of the moldavite parent mixture from the OSM sand average value of 15.3% to the moldavite average value of 11.5% would require addition (and full isotope homogenization) of a much higher proportion of meteoric water. The mid-Miocene climate of this part of Europe was significantly warmer than modern climate^{60, 61} and the average $\delta^{18}\text{O}$ values of Miocene meteoric water were also higher, most probably in the range $-5.6 \pm 0.7\%$ (ref. ⁶²). This higher $\delta^{18}\text{O}$ value would further increase the necessary proportion of fully homogenized meteoric water to unrealistic levels at ~ 30 – 40 vol.% of the mixture.

The Fig. 2 clearly shows that the carbonate-rich OSM sediment types could not have been an important component in the moldavite parent mixture. The OSM sands and clayey sands, with only a minor carbonate component, are much more suitable with respect to both major element chemistry and O isotope composition. Correlations between the major element contents and $\delta^{18}\text{O}$ are generally poor (Fig. 3). The dolomitic carbonate, present as a minor clastic component in some types of OSM sands⁴, was clearly present but only at quantities of a few per cent, at

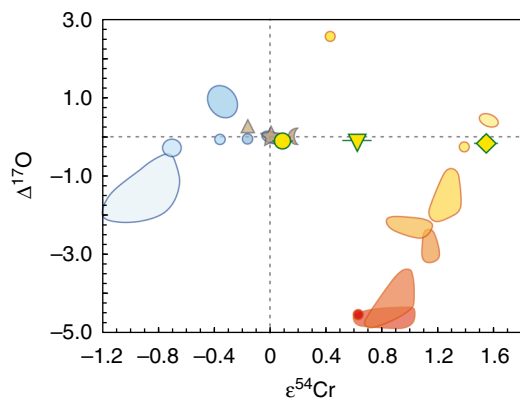


Fig. 4 $\Delta^{17}\text{O}$ vs. $\epsilon^{54}\text{Cr}$ in impact glasses and tektites from this study compared with chondrites, achondrites and large planetary bodies. The plot is modified from refs. ^{3, 26, 58} with new data from this study plotted as yellow symbols (circle—SBM-88; reversed triangle—IR-7; diamond—IR-8), with 2 s.e. uncertainties plotted. For oxygen, the error bars are smaller than the corresponding symbol size. Different hues of orange from light to dark represent different classes of carbonaceous chondrites (CI, Tagish Lake, CR, CB, CM, CV, CO, CK—red spot), the single point with high $\Delta^{17}\text{O}$ -2.5‰ represents Rumuruti chondrites. Different hues of blue from light to dark represent ureilites (farthest from Earth), mesosiderites-HED meteorites-pallasites-IIIAB irons group, ordinary chondrites, aubrites, angrites and enstatite chondrites (near-identical to Earth). Triangle—Mars; star—Earth; crescent—Moon

maximum⁶³. Such a small admixture of high- $\delta^{18}\text{O}$ carbonate was thus only one of several factors controlling the $\delta^{18}\text{O}$ range of moldavites. The carbonate as an important source component is also ruled out from high $^{87}\text{Sr}/^{86}\text{Sr}$ ratios in moldavites^{42, 64}, which indicate that a major part of Sr in moldavites is derived from silicates rather than from clastic carbonates. Similarly, the documented mass-independent effects⁶⁵ during high-temperature decomposition of carbonates would have only a limited effect on $\Delta^{17}\text{O}$ of moldavites as evidenced by the measured values which are not shifted from the common crustal range.

Therefore, it can be assumed that the observed $\delta^{18}\text{O}$ values of moldavites resulted from a combination of several factors: (i) mixing of quartz, clay, carbonate and some other minor components in varying proportions; (ii) addition of ~10–30 vol.% of water into the parent mixture; and (iii) isotope fractionation between the molten glass and separated volatiles at temperatures above 1200 °C. These findings are also supported by moderate to significant losses of highly and moderately volatile elements^{4, 13, 41, 66–68}, while less volatile elements appear to have been quantitatively transported into moldavite melts without accompanying isotope fractionation^{57, 63, 69}. Unfortunately, the O isotope fractionations for the gas phase-melt systems are not calibrated in the temperature range of interest (i.e., between the melting temperature of moldavite glass and that of lechatelierite, generally above 1200 °C). By projection of the available fractionations⁷⁰ into this high-temperature region it can be assumed that escaping volatiles (mainly CO, CO₂) should have their $\delta^{18}\text{O}$ values several tenths or a few per mil units higher than the silicate melt, shifting the residual melt $\delta^{18}\text{O}$ to a lower values.

In contrast to a resolved difference in $\delta^{18}\text{O}$ between moldavites and their inferred parent materials (this study and refs. ^{41, 51}), overlapping O isotope compositions were found for the Ivory Coast tektites, and their likely parental metasedimentary rocks and granitic dykes in the Bosumtwi impact structure, Ghana⁷¹. Therefore, the magnitude of the $\delta^{18}\text{O}$ shift observed during tektite formation can perhaps be related to the quantity of volatile-bearing species (water, carbonates and organic matter)

Table 2 Chromium isotope systematics of impact-related materials from this study

	Cr (p.p.m.)	$\epsilon^{53}\text{Cr}$	2 s.e.	$\epsilon^{54}\text{Cr}$	2 s.e.	n
<i>Irghizites and splash forms</i>						
IR-8	213 ^a	0.31	0.03	1.54	0.08	4
IR-7	122 ^a	0.15	0.05	0.62	0.10	2
<i>Tektites</i>						
SBM-88	50 ^b	0.01	0.04	0.09	0.07	4
<i>Terrestrial reference materials</i>						
BHVO-2	280 ^c	0.02	0.03	0.07	0.07	2

The letter n represents the number of individual runs where each single run consists of four successive measurements in static mode with isotopes shifted by one mass unit in the Faraday detectors
^aData from ref. ²⁸
^bData from ref. ⁵⁷
^cCertified value from US Geological Survey

present in the target area. Such an observation implies that solely the transformation of target materials into tektites does not generate mass-independent effects and other pertinent processes are required to modify $\Delta^{17}\text{O}$.

Unlike the constrained crustal-like $\Delta^{17}\text{O}$ values reported for moldavites, oxygen isotope systematics of irghizites and splash forms from Zhamanshin show several peculiar traits. The most appealing feature of the data set are the uniformly low $\Delta^{17}\text{O}$ values in the irghizites ($\leq -0.14\text{‰}$) relative to basic splash forms ($\geq -0.10\text{‰}$) while, at the same time, irghizites display higher $\delta^{18}\text{O}$ values (Fig. 1). The difference in chemical composition between irghizites and basic splash forms reflects differences in the composition of target materials in Zhamanshin area²⁸. Basic splash forms sampled deeper-seated lithologies such as andesitic volcanic rocks and basement tuffs, while irghizites were formed from surface sands and clays^{27, 28, 72}, evidenced also by distinct Sr–Nd isotope systematics⁶⁴ and cosmogenic ¹⁰Be identified solely in the irghizites, which suggests sampling of surface material⁷³. This provides unequivocal evidence for the depth segregation limiting the interaction between impactor and target rocks for Zhamanshin impact materials but does not explain the difference in $\Delta^{17}\text{O}$ between basic splash forms and irghizites (Fig. 1). The observation is discussed in terms of two different scenarios: the anomaly is due to admixture of anomalous oxygen from the extraterrestrial projectile, or the impact melts may have exchanged with isotopically anomalous air oxygen in the aftermath of the impact. We assume a $\delta^{18}\text{O} \approx 10\text{‰}$ for the end member target rock of irghizites, which is compatible with their sedimentary siliciclastic source⁷⁴.

The low $\Delta^{17}\text{O}$ in irghizites could be caused by contamination with anomalous (i.e., $\Delta^{17}\text{O} < -0.5\text{‰}$) oxygen from the projectile. While both chondritic and iron meteorites were proposed as possible impactors for Zhamanshin^{27, 28, 36}, in the context of an impactor origin of the O isotope anomaly in irghizites, ordinary chondrites and iron meteorites would be excluded as impactor. Addition of ~2–10% oxygen from a carbonaceous chondrite impactor would explain the O isotope systematics of irghizites but most classes of carbonaceous chondrites were excluded on the basis of siderophile element systematics²⁸. The abundances of highly siderophile (HSE—Os, Ir, Ru, Pt, Pd, Re) and moderately siderophile (MSE—Ni, Co, Cr) elements as an indicator for impactor contribution differ greatly between irghizites and basic splash-forms²⁸. In particular, Ni, Co and Cr are enriched in irghizites relative to basic splash forms (up to ~2000 p.p.m. Ni in the former)^{27, 28, 36}, suggesting a resolved addition from a Ni-rich chondrite. To qualify the impactor more precisely, the unique ⁵⁴Cr excess of 1.54ε units found for irghizite IR-8 (Table 2 and

Fig. 4) represents the highest anomaly ever observed in any terrestrial sample, including those with resolved meteoritic addition⁵⁸, and among the highest anomalies ever reported for any Solar System material^{26, 56}. This high $\epsilon^{54}\text{Cr}$ falls in the field intermediate between CI-type chondrites and the ungrouped Tagish Lake chondrite. The observed Cr isotope composition clearly is inherited from the impactor and disqualifies most carbonaceous chondrites as an impactor for the Zhamanshin astrobleme. A simple model (Fig. 5) demonstrates that ^{54}Cr systematics in Zhamanshin impact glasses can be reproduced by mixing with 2–7% of CI chondrite having 2650 p.p.m. Cr and $\epsilon^{54}\text{Cr} = 1.7$ (refs. 56, 75). It also requires two different target lithologies with low (IR-8) and intermediate (IR-7) Cr abundance, fully consistent with recent investigations^{27, 28} and oxygen isotope constraints (this study). At present, combined ^{54}Cr – ^{17}O isotope data are only collected for a limited number of individual carbonaceous chondrites and the possibility of the existence of chondrites with yet unaccounted ^{54}Cr – ^{17}O isotope systematics is not eliminated. For example, ~5% admixture of a hypothetical Ni-rich carbonaceous chondrite with $\epsilon^{54}\text{Cr} = 1.6$ and $\Delta^{17}\text{O}$ of ~–2‰, which would fall close to the field of CR carbonaceous chondrites, would explain the observed composition of irghizites without a need for isotope exchange with Earth's atmosphere, discussed below. However, a meteorite with such an isotope signature has not yet been reported and ^{54}Cr isotope signature in particular represents a serious constraint for tracing a suitable impactor type.

The Earth's atmospheric molecular oxygen carries a $\Delta^{17}\text{O}$ value of –0.47‰ (ref. 22); with a correction of $\delta^{17}\text{O}$ (see ref. 76 for discussion). At high temperatures, a limited extent of mass-dependent isotope fractionation is expected between molecular O_2 and silicate melt so that the composition of the irghizites may represent a mixture of the target rocks and air O_2 (Fig. 1). In such a scenario, 20–35% of the oxygen in the irghizites would have equilibrated with air O_2 while it would be generally <10% for

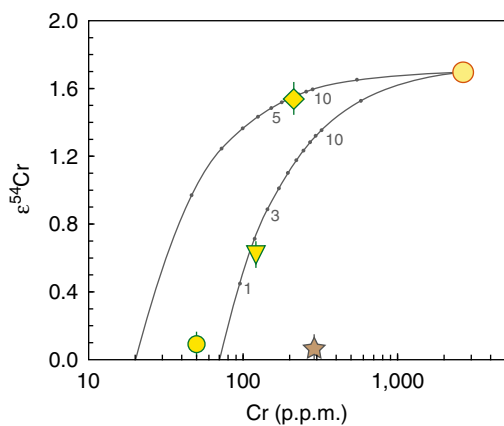


Fig. 5 Simple binary mixing model for impact glasses from Zhamanshin with CI chondrite impactor. CI chondrite with 2650 p.p.m. Cr and $\epsilon^{54}\text{Cr} = 1.7$ (yellow circle with a red rim; see main text for data sources) was mixed with different target materials, a Cr-poor (20 p.p.m.) composition for irghizite IR-8 (diamond) and intermediate-Cr (70 p.p.m.) composition for composite splash-form IR-7 (reversed triangle), reflecting their different sources²⁸. The numbers along the calculated mixing lines indicate a proportion of the impactor matter in the mixture. The ^{54}Cr results are identical to ^{53}Cr results (not shown), supporting the robust nature of the mixing process. The nil effects for moldavite SBM-88 (yellow circle with a green rim) and terrestrial standard BHVO-2 (star) are documented. The errors for $\epsilon^{54}\text{Cr}$ values are 2 s.e. (see Table 2), the errors for Cr concentrations (1–3% RSD)²⁸ are smaller than the corresponding symbol size

basic splash forms. This scenario would account for the low $\Delta^{17}\text{O}$ in irghizites compared to basic splash forms. It also supports the recent models of formation of impact glasses from Zhamanshin^{27, 28}, in which small particle-sized irghizites represent the last phase of fallback deposition, thus allowing for the extended period of time in contact with a progressively cooling and collapsing vapor cloud, in comparison with larger particles such as basic splash-forms⁷⁷. A detailed petrographic and microchemical study confirmed that mm- to cm-sized irghizite bodies frequently formed by coalescence of ~1 mm large glass droplets, a feature not observed for basic splash forms²⁸. A surface layer 0.1 mm thick represents ~50% of the volume of such a sphere. Iron in interior parts of these glass spheres is in Fe^{2+} form whereas more oxidized iron is found in surface layers. This is indicated by the observation that rims of the spheres display lower analytical totals and higher total Fe contents than their interiors. In particular, the analytical totals for the rims vary between 97 and 99 wt.% and FeO^{tot} ranges from 8.6 to 10.4 wt.%, while the inner parts of the spheres show analytical totals of ~100 wt.% with FeO^{tot} ranging from 5.6 to 7.0 wt.%. The balancing of the analytical totals in rims requires some 30–50% of total iron in rims to be present as Fe^{3+} . Apparently, lower analytical totals associated with Fe enrichment in the rims suggest the origin of rims in a more oxidizing environment than for interiors of spherules, indicating exchange with the atmosphere²⁴. We note that the measured $\Delta^{17}\text{O}$ data are from bulk homogenized irghizite samples and that in-situ $\Delta^{17}\text{O}$ values would likely vary strongly within individual irghizite bodies. The model of slow gravitational settling⁷⁷ and chemical and isotope exchange with a slowly collapsing vapor plume cannot be applied to moldavites (distal ejecta) due to their instantaneous dislocation from the area of origin.

Combining O and Cr isotope data allow both classifying the impactor type and pinpointing the process, which gives rise to the unusually low $\Delta^{17}\text{O}$ in irghizites. The $\Delta^{17}\text{O}$ of both CI carbonaceous chondrites and Tagish Lake chondrite is close to the terrestrial fractionation line. The Cr concentration in irghizite IR-8 is 213 p.p.m., whereas it is presumably low (~20 p.p.m.) in possible target lithologies²⁸. The ^{54}Cr systematics indicates that >90% of Cr is derived from the impactor (Fig. 5), and the general ^{54}Cr systematics disqualifies most types of carbonaceous chondrites (Fig. 4). Mixing a target material ($\delta^{18}\text{O} = 10\text{‰}$; $\Delta^{17}\text{O} = -0.09\text{‰}$) with a CI-like impactor having $\delta^{18}\text{O} = 16.3\text{‰}$ and $\Delta^{17}\text{O} = 0.2 \pm 0.2\text{‰}$ (ref. 78) (Tagish Lake chondrite has a similar composition) would not result in the observed low $\Delta^{17}\text{O}$ of the irghizites. Therefore, we conclude that exchange with atmospheric O_2 in a vapor plume could lead to the observed low $\Delta^{17}\text{O}$ in irghizites. Apart from rare sulphates⁷⁹ and fossil biominerals^{80, 81}, this makes irghizites of the Zhamanshin astrobleme one of the few terrestrial materials in the geological record that carries traces of the isotope anomaly of air O_2 .

Methods

Oxygen purification and isotope measurements. The procedures for the oxygen extraction and high-precision triple-oxygen isotope measurements followed the methodology outlined elsewhere⁵⁴. In brief, ~2 mg of a powdered sample were reacted with fluorine gas at a low pressure (~20 mbar) and heated with a CO_2 -based laser. Excess fluorine was removed by hot NaCl and chlorine was subsequently trapped with liquid nitrogen cold trap. Oxygen liberated from analyzed samples was collected on 5 Å molecular sieves and cleaned by gas chromatography for mass spectrometry analysis. For some samples, oxygen was extracted using an improved protocol that applies BrF_5 as the fluorinating agent (details of this protocol are given elsewhere⁷⁶). All three oxygen isotopes were measured using a Finnigan MAT 253 gas source mass spectrometer, housed at the Göttingen University. The results are reported in $\delta^{17}\text{O}$ – $\delta^{18}\text{O}$ (‰) notation and $\Delta^{17}\text{O}$ (‰) values relative to VSMOW2 reference material. The $\Delta^{17}\text{O}$ is defined relative to a reference line with the slope of 0.5305 and zero intercept⁵⁴ as $\Delta^{17}\text{O} = 1000\ln(\delta^{17}\text{O}/1000 + 1) - 0.5305 \times 1000\ln(\delta^{18}\text{O}/1000 + 1)$, with San Carlos olivine having a $\Delta^{17}\text{O} = -0.05\text{‰}$ (ref. 76). The 1 s.d. reproducibility of the measurements was always better than 0.3‰ for $\delta^{18}\text{O}$ and 0.01‰ for $\Delta^{17}\text{O}$ values, respectively, based on repeated

analyses of reference quartz NBS-28 (National Bureau of Standards, USA) and San Carlos olivine.

Chromium purification and isotope measurements. The procedures for the Cr isotope measurements were performed at the Institut de Physique du Globe de Paris, France. The two irghizite samples (IR-7 and IR-8), one moldavite sample (SBM-88) as well as the basalt BHVO-2 (Hawaii, USA) were dissolved in a mixture of concentrated HF and HNO₃ in Teflon bombs at 140 °C for several days until complete dissolution of all phases. Chromium was purified by cation exchange chromatography following the method described elsewhere⁵⁵. The ⁵³Cr/⁵²Cr and ⁵⁴Cr/⁵²Cr isotope ratios were measured using a Triton thermal ionization mass spectrometer (Fisher Scientific, Bremen, Germany) following the method described elsewhere²⁶. Briefly, samples were loaded in chloride form on the outgassed W filaments together with an Al-silicagel–H₃BO₃ emitter. Each run comprised 20 blocks of 20 cycles and each single run was a combination of three successive multi-collection measurements in static mode. The measured ⁵³Cr/⁵²Cr and ⁵⁴Cr/⁵²Cr ratios are reported in $\epsilon^{53}\text{Cr}$ and $\epsilon^{54}\text{Cr}$ notation (1 in 10,000 difference relative to NIST SRM 3112a reference material) and were normalized using an exponential law to ⁵²Cr/⁵⁰Cr = 19.28323 (ref. ⁸²). Each sample was measured two to four times (Table 2).

Data availability. All relevant data are available from the authors on request and/or are included with the manuscript in the form of data tables and data within figures.

Received: 1 September 2016 Accepted: 8 June 2017

Published online: 09 August 2017

References

- Remusat, L. Organic material in meteorites and the link to the origin of life. *BIO Web Conf* **2**, 03001–03010 (2014).
- Koebel, C. in *Treatise on Geochemistry* 2nd edn, Vol. 2 (ed. Davis, A. M.) 73–118 (Elsevier Ltd., 2014).
- Krot, A. N., Keil, K., Scott, E. R. D., Goodrich, C. A. & Weisberg, M. K. in *Treatise on Geochemistry*, 2nd edn, Vol. 1 (ed. Davis, A. M.) 1–63 (Elsevier Ltd., 2014).
- Žák, K. et al. Chemistry of tertiary sediments in the surroundings of the Ries impact structure and moldavite formation revisited. *Geochim. Cosmochim. Acta* **179**, 287–311 (2016).
- Trinquier, A., Birck, J.-L. & Allège, C. J. The nature of the KT impactor. A ⁵⁴Cr reappraisal. *Earth Planet. Sci. Lett.* **241**, 780–788 (2006).
- Koebel, C. & Shirey, S. B. Detection of a meteoritic component in Ivory Coast tektites with rhenium-osmium isotopes. *Science* **261**, 595–598 (1993).
- Vickery, A. M. The theory of jetting: application to the origin of tektites. *Icarus* **105**, 441–453 (1993).
- Friedman, I. The water, deuterium, gas and uranium content of tektites. *Geochim. Cosmochim. Acta* **14**, 316–322 (1958).
- Beran, A. & Koebel, C. Water in tektites and impact glasses by Fourier-transformed infrared spectrometry. *Meteorit. Planet. Sci.* **32**, 211–216 (1997).
- Watt, N., Bouchet, R. A. & Lee, C.-T. A. Exploration of tektite formation processes through water and metal content measurements. *Meteorit. Planet. Sci.* **46**, 1025–1032 (2011).
- Žák, K., Skála, R., Řanda, Z. & Mizera, J. A review of volatile compounds in tektites, and carbon content and isotopic composition of moldavite glass. *Meteorit. Planet. Sci.* **47**, 1010–1028 (2012).
- Stöffler, D., Artemieva, N. A. & Pierazzo, E. Modeling the Ries-Steinheim impact event and the formation of the moldavite strewn field. *Meteorit. Planet. Sci.* **37**, 1893–1907 (2002).
- von Engelhardt, W., Berthold, C., Wenzel, T. & Dehner, T. Chemistry, small-scale inhomogeneity, and formation of moldavites as condensates from sands vaporized by the Ries impact. *Geochim. Cosmochim. Acta.* **69**, 5611–5626 (2005).
- Melosh, H. J. & Artemieva, N. How does tektite glass lose its water? *Lunar Planet. Sci.* **35**, #1723 (2004).
- Artemieva, N. Tektites: model versus reality. *Lunar Planet. Sci.* **XXXIX**, 1651 (2008).
- Melosh, H. J. & Vickery, A. M. Melt droplet formation in energetic impact events. *Nature* **350**, 494–497 (1991).
- Johnson, B. C. & Melosh, H. J. Formation of spherules in impact produced vapor plumes. *Icarus* **217**, 416–430 (2012).
- Johnson, B. C. & Melosh, H. J. Formation of melt droplets, melt fragments, and accretionary impact lapilli during a hypervelocity impact. *Icarus* **228**, 347–363 (2014).
- Clayton, R. N. in *Treatise on Geochemistry* Vol. 1 (ed. Davis, A. M.) 129–142 (Elsevier Ltd., 2003).
- Clayton, R. N. & Mayeda, T. K. Oxygen isotope studies of achondrites. *Geochim. Cosmochim. Acta* **60**, 1999–2017 (1996).
- Franchi, I. A., Wright, I. P., Sexton, A. S. & Pillinger, C. T. The oxygen-isotopic composition of Earth and Mars. *Meteorit. Planet. Sci.* **34**, 657–661 (1999).
- Young, E. D., Yeung, L. Y. & Kohl, I. E. On the $\Delta^{17}\text{O}$ budget of atmospheric O₂. *Geochim. Cosmochim. Acta* **135**, 102–125 (2014).
- Thiemens, M. H. History and applications of mass-independent isotope effects. *Annu. Rev. Earth. Planet. Sci.* **34**, 217–262 (2006).
- Engrand, C. et al. Isotopic compositions of oxygen, iron, chromium, and nickel in cosmic spherules: toward a better comprehension of atmospheric entry heating effects. *Geochim. Cosmochim. Acta* **69**, 5365–5385 (2005).
- Trinquier, A., Birck, J.-L. & Allège, C. J. Widespread ⁵⁴Cr heterogeneity in the inner solar system. *Astrophys. J.* **655**, 1179–1185 (2007).
- Göpel, C., Birck, J.-L., Galy, A., Barrat, J.-A. & Zanda, B. Mn–Cr systematics in primitive meteorites: insights from mineral separation and partial dissolution. *Geochim. Cosmochim. Acta* **156**, 1–24 (2015).
- Mizera, J., Řanda, Z. & Tomandl, I. Geochemical characterization of impact glasses from the Zhamanshin crater by various modes of activation analysis. Remarks on genesis of irghizites. *J. Radioanal. Nucl. Chem.* **293**, 359–376 (2012).
- Jonášová, Š. et al. Geochemistry of impact glasses and target rocks from the Zhamanshin Impact Structure, Kazakhstan: Implications for mixing of target and impactor matter. *Geochim. Cosmochim. Acta.* **190**, 239–264 (2016).
- Skála, R., Strnad, L., McCammon, C. & Čada, M. Moldavites from the Cheb Basin, Czech Republic. *Geochim. Cosmochim. Acta* **73**, 1145–1179 (2009).
- Stöffler, D. et al. Ries crater and suevite revisited—observations and modeling Part I: observations. *Meteorit. Planet. Sci.* **48**, 515–589 (2013).
- Buchner, E., Schmieder, M., Schwarz, W. H. & Trierloff, M. Das Alter des Meteoritenkraters Nördlinger Ries—eine Übersicht und kurze Diskussion der neueren Datierungen des Riesimpakts. *Z. Dt. Ges. Geowiss.* **164**, 433–445 (2013).
- Vetvicka, I., Frank, J. & Drtina, J. Electron microprobe analysis (WDS EPMA) of Zhamanshin glass reveals the impactor and a common role of accretion in the origin of splash-form impact glass. *IOP Conf. Ser.: Mater. Sci. Eng.* **7**, 012029 (2010).
- Florenskii, P. V. & Dabizha, A. I. *Meteoritnyi Krater Zhamanshin (In Russian)* 128 (Nauka, 1980).
- Florenski, P. W. Der Meteoritenkrater Zhamanshin (nordliches Aralgebiet UdSSR) und seine Tektite und Impaktite. *Chem. Erde.* **36**, 83–95 (1977).
- Fredriksson, K., de Gasparis, A. & Ehrmann, W. D. The Zhamanshin structure: chemical and physical properties of selected samples. *Meteoritics* **12**, 229–230 (1977).
- Palme, H., Grieve, R. A. F. & Wolf, R. Identification of the projectile at the Brent crater, and further considerations of projectile types at terrestrial craters. *Geochim. Cosmochim. Acta* **45**, 2417–2424 (1981).
- von Heide, K. & Schmidt, H.-G. Über das thermische Entgasungsverhalten und den Gasgehalt der Irghisite. *Chem. Erde.* **37**, 271–273 (1978).
- von Heide, K., Brückner, H.-P., Schmidt, H.-G. & Florenski, P. W. Untersuchungen zum Gasgehalt der Irghisite und Zhamanshinite. *Chem. Erde.* **40**, 340–351 (1981).
- Delano, J. W., Bouška, V. & Řanda, Z. in *2nd International Conference on Natural Glasses* (ed. Konta, J.) 221–230 (Charles University, Prague, Czech Republic, 1988).
- Bouška, V., Benada, J., Řanda, Z. & Kuncíř, J. Geochemical evidence for the origin of moldavites. *Geochim. Cosmochim. Acta* **37**, 121–131 (1973).
- von Engelhardt, W., Luft, E., Arndt, J., Schock, H. & Weiskirchner, W. Origin of moldavites. *Geochim. Cosmochim. Acta* **51**, 1425–1443 (1987).
- Horn, P., Müller-Sohnius, D., Köhler, H. & Graup, G. Rb–Sr systematics of rocks related to the Ries Crater, Germany. *Earth Planet. Sci. Lett.* **72**, 384–392 (1985).
- Luft, E. *Zur Bildung der Moldavite beim Ries-Impact aus Tertiären Sedimenten* 202 (Enke Verlag, 1983).
- Řanda, Z., Mizera, J., Frána, J. & Kučera, J. Geochemical characterization of moldavites from a new locality, the Cheb Basin, Czech Republic. *Meteorit. Planet. Sci.* **43**, 461–477 (2008).
- Meisel, T., Lange, J.-M. & Krähenbühl, U. The chemical variation of moldavite tektites: simple mixing of terrestrial sediments. *Meteorit. Planet. Sci.* **32**, 493–502 (1997).
- Trnka, M. & Houzar, S. Moldavites: a review. *Bull. Czech. Geol. Surv.* **77**, 283–302 (2002).
- Schwarz, W. H. & Lippolt, H. J. ⁴⁰Ar–³⁹Ar step-heating of impact glasses from the Nördlinger Ries impact crater—Implications on excess argon in impact melts and tektites. *Meteorit. Planet. Sci.* **49**, 1023–1036 (2014).
- Palme, C., Janssens, M.-J., Takahashi, H. A. E. & Hertogen, J. Meteoritic material at five large impact craters. *Geochim. Cosmochim. Acta* **42**, 313–323 (1978).
- Schmidt, G. & Pernicka, E. The determination of platinum group elements (PGE) in target rocks and fall-back material of the Nördlinger Ries impact crater, Germany. *Geochim. Cosmochim. Acta* **58**, 5083–5090 (1994).

50. Ackerman, L. et al. The behavior of osmium and other siderophile elements during impacts: Insights from the Ries impact structure and central European tektites. *Geochim. Cosmochim. Acta* **210**, 59–70 (2017).
51. Taylor, H. P. Jr. & Epstein, S. Correlations between O^{18}/O^{16} ratios and chemical compositions of tektites. *J. Geophys. Res.* **74**, 6834–6844 (1969).
52. Taylor, H. P. Jr. & Epstein, S. Oxygen isotope studies on the origin of tektites. *J. Geophys. Res.* **67**, 4485–4490 (1962).
53. Taylor, H. P. Jr. & Epstein, S. Oxygen isotope studies of Ivory Coast tektites and impactite glass from the Bosumtwi Crater, Ghana. *Science* **153**, 173–175 (1966).
54. Pack, A. & Herwartz, D. The triple oxygen isotope composition of the Earth mantle and understanding $D^{17}O$ variations in terrestrial rocks and minerals. *Earth Planet. Sci. Lett.* **390**, 138–145 (2014).
55. Trinquier, A., Birck, J.-L., Allègre, C. J., Gopel, C. & Ulfbeck, D. Mn-53-Cr-53 systematics of the early solar system revisited. *Geochim. Cosmochim. Acta* **72**, 5146–5163 (2008).
56. Qin, L., Alexander, C. M. O. D., Carlson, R. W., Horan, M. F. & Yokoyama, T. Contributors to chromium isotope variation of meteorites. *Geochim. Cosmochim. Acta* **74**, 1122–1145 (2010).
57. Magna, T. et al. Lithium in tektites and impact glasses: implications for sources, histories and large impacts. *Geochim. Cosmochim. Acta* **75**, 2137–2158 (2011).
58. Mougél, B., Moynier, F., Göpel, C. & Koeberl, C. Chromium isotope evidence in ejecta deposits for the nature of Paleoproterozoic impactors. *Earth Planet. Sci. Lett.* **460**, 105–111 (2017).
59. Vennemann, T. W., Morlok, A., von Engelhardt, W. & Kyser, K. Stable isotope composition of impact glasses from the Nördlinger Ries impact crater, Germany. *Geochim. Cosmochim. Acta* **65**, 1325–1336 (2001).
60. Utescher, T., Bruch, A. A., Micheels, A., Mosbrugger, V. & Popova, S. Cenozoic climate gradients in Eurasia—a palaeo-perspective on future climate change? *Palaeogeograph. Palaeoclimat. Palaeoecol.* **304**, 351–358 (2011).
61. Foster, G. L., Lear, C. H. & Rae, J. W. B. The evolution of pCO_2 , ice volume and climate during the middle Miocene. *Earth Planet. Sci. Lett.* **341–344**, 243–254 (2012).
62. Tütken, T. & Vennemann, T. Stable isotope ecology of Miocene large mammals from Sandelzhausen, southern Germany. *Paläontol. Z.* **83**, 207–226 (2009).
63. Rodovská, Z. et al. The fate of moderately volatile elements in impact events—lithium connection between the Ries sediments and central European tektites. *Meteorit. Planet. Sci.* **51**, 2403–2415 (2016).
64. Shaw, H. F. & Wasserburg, G. J. Age and provenance of the target materials for tektites and possible impactites as inferred from Sm-Nd and Rb-Sr systematics. *Earth Planet. Sci. Lett.* **60**, 155–177 (1982).
65. Miller, M. F. et al. Mass-independent fractionation of oxygen isotopes during thermal decomposition of carbonates. *Proc. Natl Acad. Sci. USA* **99**, 10988–10993 (2002).
66. Rodovská, Z. et al. Implications for behavior of volatile elements during impacts—zinc and copper systematics in sediments from the Ries impact structure and central European tektites. *Meteorit. Planet. Sci.* doi:doi:10.1111/maps.12922.
67. Moynier, F. et al. Isotopic fractionation of zinc in tektites. *Earth Planet. Sci. Lett.* **277**, 482–489 (2009).
68. Moynier, F., Koeberl, C., Beck, P., Jourdan, F. & Telouk, P. Isotopic fractionation of Cu in tektites. *Geochim. Cosmochim. Acta* **74**, 799–807 (2010).
69. Humayun, M. & Koeberl, C. Potassium isotopic composition of Australasian tektites. *Meteorit. Planet. Sci.* **39**, 1509–1516 (2004).
70. Beaudoin, G. & Therrien, P. in *Handbook of Stable Isotope Analytical Techniques* vol. II (ed. de Groot, P. A.) 1120–1122 (Elsevier Ltd., 2009).
71. Koeberl, C., Reimold, W. U., Blum, J. D. & Chamberlain, C. P. Petrology and geochemistry of target rocks from the Bosumtwi impact structure, Ghana, and comparison with Ivory Coast tektites. *Geochim. Cosmochim. Acta* **62**, 2179–2196 (1998).
72. Bouška, V., Povondra, P., Florenskij, P. V. & Řanda, Z. Irghizites and zhamanshinites: Zhamanshin crater, USSR. *Meteoritics* **16**, 171–184 (1981).
73. Raisbeck, G. M., Yiou, F., Zhou, S. Z. & Koeberl, C. ^{10}Be in irghizite and zhamansinite impact glasses. *Chem. Geol.* **70**, 120 (1988).
74. Taylor, H. P. J. & Sheppard, S. M. F. Igneous rocks: I. Processes of isotopic fractionation and isotope systematics. *Rev. Mineral.* **16**, 227–271 (1986).
75. Lodders, K. & Fegley, B. *The Planetary Scientist's Companion*. 400 (Oxford University Press, 1998).
76. Pack, A. et al. The oxygen isotope composition of San Carlos olivine on VSMOW2-SLAP2 scale. *Rapid Commun. Mass Spectrom.* **30**, 1495–1504 (2016).
77. Schedl, A. Searching for distal ejecta on the craton: the sedimentary effects of meteorite impact. *J. Geol.* **123**, 201–232 (2015).
78. Clayton, R. N. & Mayeda, T. K. The oxygen isotope record in Murchison and other carbonaceous chondrites. *Earth Planet. Sci. Lett.* **67**, 151–161 (1984).
79. Bao, H., Lyons, J. R. & Zhou, C. Triple oxygen isotope evidence for elevated CO_2 levels after a Neoproterozoic glaciation. *Nature* **453**, 504–506 (2008).
80. Gehler, A., Gingerich, P. D. & Pack, A. Temperature and atmospheric CO_2 concentration estimates through the PETM using triple oxygen isotope analysis of mammalian bioapatite. *Proc. Natl Acad. Sci. USA* **113**, 7739–7744 (2016).
81. Pack, A., Gehler, A. & Süssenberger, A. Exploring the usability of isotopically anomalous oxygen in bones and teeth as paleo- CO_2 -barometer. *Geochim. Cosmochim. Acta* **102**, 306–317 (2013).
82. Shields, W. R., Murphy, T. J., Catanzaro, E. J. & Garner, E. L. Absolute isotopic abundance ratios and the atomic weight of a reference sample of chromium. *J. Res. Natl. Bur. Stand.* **70A**, 193–197 (1966).
83. Philpotts, J. A. & Pinson, W. H. Jr. New data on the chemical composition and origin of moldavites. *Geochim. Cosmochim. Acta* **30**, 253–266 (1966).

Acknowledgements

This study was supported by the Czech Science Foundation project 13-22351S. F.M. thanks the ERC under the European Community's H2020 framework program/ERC grant agreement #637503 (Pristine), the ANR for a chaire d'Excellence Sorbonne Paris Cité (IDEX13C445) and the UnivEarthS Labex program (ANR-10-LABX-0023 and ANR-11-IDEX-0005-02). Part of this work was supported by IGP multidisciplinary program PARI, and by Region ile-de-France SESAME Grant no. 12015908.

Author contributions

T.M. and K.Ž. conceived the study. R.S., J.M. and Z.Ř. provided the samples. A.P., S.P., F.M. and B.M. collected the data. Š.J. and R.S. characterized the microchemistry of key samples. All authors contributed to data interpretation. T.M., K.Ž., A.P. and F.M. took lead in writing.

Additional information

Supplementary Information accompanies this paper at doi:10.1038/s41467-017-00192-5.

Competing interests: The authors declare no competing financial interests.

Reprints and permission information is available online at <http://npg.nature.com/reprintsandpermissions/>

Publisher's note: Springer Nature remains neutral with regard to jurisdictional claims in published maps and institutional affiliations.



Open Access This article is licensed under a Creative Commons Attribution 4.0 International License, which permits use, sharing, adaptation, distribution and reproduction in any medium or format, as long as you give appropriate credit to the original author(s) and the source, provide a link to the Creative Commons license, and indicate if changes were made. The images or other third party material in this article are included in the article's Creative Commons license, unless indicated otherwise in a credit line to the material. If material is not included in the article's Creative Commons license and your intended use is not permitted by statutory regulation or exceeds the permitted use, you will need to obtain permission directly from the copyright holder. To view a copy of this license, visit <http://creativecommons.org/licenses/by/4.0/>.

© The Author(s) 2017